Medical Physics
The International Journal of Medical Physics Research and Practice

In vivo dosimetry with optically stimulated luminescent dosimeters, OSLDs, compared to diodes; the effects of buildup cap thickness and fabrication material

Paul A. Jursinic and Clifford J. Yahnke

Citation: Medical Physics **38**, 5432 (2011); doi: 10.1118/1.3633939
View online: http://dx.doi.org/10.1118/1.3633939
View Table of Contents: http://scitation.aip.org/content/aapm/journal/medphys/38/10?ver=pdfcov
Published by the American Association of Physicists in Medicine

In vivo dosimetry with optically stimulated luminescent dosimeters, OSLDs, compared to diodes; the effects of buildup cap thickness and fabrication material

Paul A. Jursinic[a)]
West Michigan Cancer Center, 200 North Park St. Kalamazoo, Michigan 49007

Clifford J. Yahnke
Landauer, Inc., 2 Science Road, Glenwood, Illinois 60425

(Received 19 May 2011; revised 11 August 2011; accepted for publication 15 August 2011; published 16 September 2011)

Purpose: For external beam *in vivo* measurements, the dosimeter is normally placed on the patient's skin, and the dose to a point of interest inside the patient is derived from surface measurements. In order to obtain accurate and reliable measurements, which correlate with the dose values predicted by a treatment planning system, a dosimeter needs to be at a point of electronic equilibrium. This equilibrium is accomplished by adding material (buildup) above the detector. This paper examines the use of buildup caps in a clinical setting for two common detector types: OSLDs and diodes. Clinically built buildup-caps and commercially available hemispherical caps are investigated. The effects of buildup cap thickness and fabrication material on field-size correction factors, C_{FS}, are reported, and differences between the effects of thickness and fabrication material are explained based on physical parameters.

Methods: Measurements are made on solid water phantoms for 6 and 15 MV x-ray beams. Two types of dosimeters are used: OSLDs, InLight/OSL Nanodot dosimeters (Landauer, Inc., Glenwood, IL) and a P-type surface diode (Standard Imaging, Madison, WI). Buildup caps for these detectors were fabricated out of M3, a water-equivalent material, and sheet-metal stock of Al, Cu, and Pb. Also, commercially available hemispherical buildup caps made of plastic water and brass (Landauer, Inc., Glenwood, IL) were used with Nanodots. OSLDs were read with an InLight microStar reader (Landauer, Inc., Glenwood, IL). Dose calculations were carried out with the XiO treatment planning system (CMS/Elekta, Stockholm) with tissue heterogeneity corrections.

Results: For OSLDs and diodes, when measurements are made with no buildup cap a change in C_{FS} of 200% occurs for a field-size change from 3 cm × 3 cm to 30 cm × 30 cm. The change in C_{FS} is reduced to about 4% when a buildup cap with wall thickness equal to the depth of maximum dose is used. Buildup caps with larger wall thickness do not cause further reduction in C_{FS}. The buildup cap fabrication material has little or no effect on C_{FS}. The perturbation to the delivered dose caused by placing a detector with a buildup cap on the surface of a patient is measured to be 4%–7%. A comparison between calculated dose and dose measured with a Nanodot and a diode for 6 and 15 MV x-rays is made. When C_{FS} factors are carefully determined and applied to measurements made on a phantom, the differences between measured and calculated doses were found to be between ±1.3%.

Conclusions: OSLDs and diodes with appropriate buildup caps can be used to measure dose on the surface of a patient and predict the delivered dose to depth dmax in a range of ±1.3% for 100 cGy. The buildup cap: can be fabricated from any material examined in this work, is best with wall thickness dmax, and causes a perturbation to the delivered dose of 4%–7% when the wall thickness is dmax. OSLDs and diodes with buildup caps can both give accurate measurements of delivered dose. [DOI: 10.1118/1.3633939]

Key words: optically stimulated luminescent dosimeters, OSLD, diodes, *in vivo* dosimetry, buildup caps

I. INTRODUCTION

A major responsibility for a medical physicist is to insure that the prescribed dose is correctly delivered to the patient. *In vivo* dosimetry is a patient specific measurement, not just a calculation check, that is, a supplement to a more general quality assurance program in the clinic.[1–5] Additionally, *in vivo* measurements document that treatment was delivered as prescribed and calculated for the treatment fractions in which the measurements are made.

In order to prevent major treatment errors and to assure high accuracy in dose delivery from complex and conformal therapy-techniques, the AAPM TG-40 recommends[6] that clinics "should have access to TLD or other *in vivo* systems."

Thermoluminescent dosimeters (TLDs) and silicon diodes have been widely used to do *in vivo* dosimetry. TLD

dosimetry has been used for over 30 years and is a proven technology.[4,7,8] PN junction-type diodes[9,10] or MOSFET detectors[11] have become very popular due to their immediate readout and high sensitivity (over 18 000 times that of an air-filled ionization chamber of the same volume).[8,12,13] With care, diodes can have higher accuracy and precision than TLDs.[14]

Over the past couple of decades, synthetic materials that exhibit the property of thermally and optically stimulated luminescence have been developed.[15,16] Man made sapphire, α-Al_2O_3:C, has characteristics that make it a good *in vivo* dosimeter: 30–60 times the sensitivity to radiation as LiF:Mg,Ti TLDs,[17] low levels of signal fading,[18–22] and an effective atomic number[17] of 11.28. A number of papers have been published recently that describe the use of OSLDs in radiation oncology clinical measurements.[19,21–26]

For external beam *in vivo* measurements, all of these dosimeters are placed on the patient's skin. To measure the surface dose the dosimeter should have a minimum of buildup material around it to avoid perturbing the surface dose.

The dose to a point of interest inside the patient must also be derived from the dose measurement at the surface. A critical but often overlooked requirement in making reliable and accurate measurements in MV beams is that the dosimeter must be near a point of electronic equilibrium. This condition is clinically realized by placing an amount of tissue equivalent material above the detector. This material is typically composed of water-equivalent plastic that is shaped into a hemispherical or cylindrical cap to facilitate placement onto a patient while providing some amount of angular symmetry. These commercial devices are commonly referred to as buildup caps. Buildup material is typically added to bring the dosimeter to dmax, the depth of maximum dose. Standard dosimetric calculations are carried out to determine the dose at depths besides that of dmax.

Generally diodes that are packaged in buildup caps designated for use over a range of x-ray energies, are placed on the surface of the patient, and are related to dose delivered at the depth of maximum dose.[9,27] There are reports in the literature[13,28–30] of use of diodes that had insufficient buildup caps. It was shown that correction factors were larger and more variable when buildup caps were inadequate. It has also been shown[31] that the measurement of collimator scatter with a columnar-miniphantom depends on the atomic number of the fabrication material of the miniphantom. A columnar-miniphantom is a cylindrical builup cap with depth and wall thickness sufficient to stop electron contamination while minimizing scatter dose.[32]

TLDs (Ref. 7) and OSLDs (Ref. 19) have little intrinsic buildup and are ideal detectors for surface dose. For OSLDs to be related to the dose delivered at dmax they must be fitted with suitable buildup caps. The question to be answered in this work is how different buildup caps affect the dose measured on the surface of a phantom and how it relates to the dose delivered at dmax. The field-size correction factor, C_{FS}, for OSLD dosimeters is studied. The effects of buildup cap thickness and fabrication material on C_{FS} are reported, and comparisons are made with diode measurements.

II. CALCULATION FORMALISM

One method for making *in vivo* measurements is the use of a detector at the surface of the patient with a buildup cap equivalent to dmax.[9] The detector reading at the surface can be converted to dose at dmax[33,34] or to any depth in a patient.[5] The detector can be calibrated in reference conditions on the surface of a phantom[33–35] or positioned away from scattering objects[5] with a cylindrical buildup cap of thickness dmax. The general equation that relates the detector reading, R, to the measurement of the dose at depth dmax in the patient in nonreference conditions, $D_{d\max}$, to measurements in reference conditions is the following:[33,34]

$$D_{d\max} = R \times N_{cal} \times \Pi i C_i \tag{1}$$

where N_{cal} is the detector calibration factor under reference conditions and C_i are correction factors for alterations in detector response caused by changes from calibration conditions of variables such as:[5,33–35] field size, temperature, dose-per-pulse, incident angle of radiation, physical wedges, and shielding blocks, and trays.

The correction factors are defined as ratios of dose to water to detector signals given for the measuring conditions normalized to reference conditions[28,33]

$$C_i = \frac{D_{d\max}(X)/D_{d\max}(ref)}{R(X)/R(ref)} \tag{2}$$

where $D_{d\max}(X)$ is the dose to depth dmax under conditions X, $D_{d\max}$(ref) is the dose to depth dmax under reference conditions, $R(X)$ is the detector reading under conditions X, and R(ref) is the detector reading under reference conditions. Generally, the dose at dmax is established by measurements with a calibrated ion chamber.

In this work the correction for field size is studied. The field-size correction factor is defined as follows:

$$C_{FS} = \frac{D_d(W_X)/D_d(W_{ref})}{R(W_{det\_X})/R(W_{det\_ref})} \tag{3}$$

$$\mathrm{W_{det\_ref}} = \mathrm{W_{ref}} \times \frac{\mathrm{SSD}}{\mathrm{SAD}} \quad \text{and} \quad \mathrm{W_{det\_X}} = \mathrm{W_X} \times \frac{\mathrm{SSD}}{\mathrm{SAD}}$$

where $\mathrm{W_{ref}}$ is the field size at depth d for reference conditions, $\mathrm{W_X}$ is the field size at depth d for some nonreference condition, $\mathrm{W_{det\_ref}}$ is the field size at the position of the detector for reference conditions, and $\mathrm{W_{det\_X}}$ is the field size at the position of the detector for some non-reference condition. There are two scatter environments around the detector: (1) the high scatter reference condition when the detector is surrounded by tissue equivalent material with a thickness much larger than dmax and (2) the lower scatter condition when the detector is at the surface and only surrounded by tissue equivalent material with a thickness of dmax. In the surface geometry the detector receives much less dose from

scattered radiation. C_{FS} corrects for the difference between these two scatter conditions.

III. MATERIALS AND METHODS

The x-ray beams used in this work had nominal energies of 6 and 15 MV. For these energies, respectively, the percentage depth doses of x-rays at depth of 10 cm, %dd_10_*x*, were 66.6 and 77.8, which were measured at the source-to-surface distance of 100 cm, according to the TG-51 protocol.[36] The radiation beams were generated by a Varian Trilogy (Varian Medical Systems, Milpitas, CA) linear accelerator. Absolute dose measurements were made with a cylindrical ion-chamber, model N30001 (PTW Freiburg Germany), which was calibrated at the University of Wisconsin Dosimetry Calibration Laboratory. In our clinic the calibrated output is adjusted to be 1 cGy/MU to water with a 10 cm × 10 cm field, source-to-detector distance of 100 cm, with the detector at a depth of maximum dose.

A typical setup-geometry for calibration of a detector is shown in Fig. 1. Irradiation of the detectors was done orthogonal to the front surface. A 0.5-cm-thick piece of Superflab was placed immediately over the detectors, which conformed to the irregular shapes of the detectors without incurring large air gaps. Superflab is a flexible water-equivalent material (Civco, Orange City, IA). The use of Superflab avoided the need for the slabs of solid water (Standard Imaging, Madison, WI) to be machined to fit the various detectors. Solid water slabs placed above the Superflab were of a thickness such that the detector was at a depth of maximum dose: 1.5 cm for 6 MV and 3.0 cm for 15 MV x-rays. An 8-cm-thick block of solid water was placed behind the detectors to provide backscatter of radiation.

Two types of detectors were used in this work. One type of detector was an OSLD,[37,38] InLight/OSL Nanodot dosimeter (Landauer, Inc., Glenwood, IL). The OSLDs are 7-mm diameter; 0.3-mm-thick plastic disks infused with aluminum oxide doped with carbon (Al_2O_3:C, synthetic sapphire). These disks are encased in a 10 mm × 10 mm × 2 mm light-tight plastic holder. The Nanodot has a water-equivalent

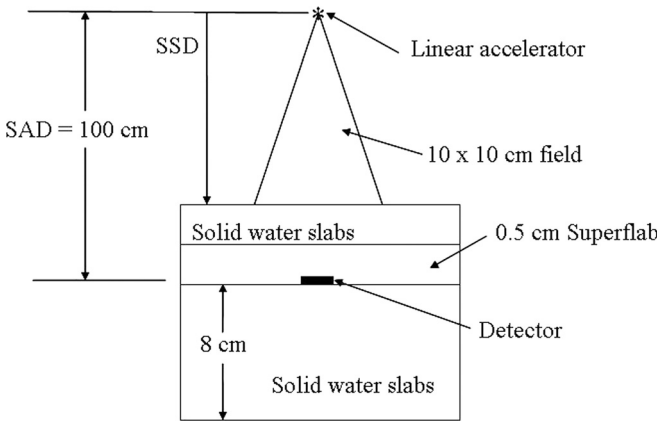

FIG. 1. The geometry used for calibrating the detectors. For 6 MV x-rays, the detector is located at a depth of 1.5 cm with an SSD of 98.5 cm. For 15 MV x-rays, the detector is located at a depth of 3.0 cm with an SSD of 97.0 cm. The lateral dimensions are 30 cm × 30 cm.

buildup[19] of 0.04 gm/cm^2. OSLDs were read with an InLight microStar reader (Landauer, Inc., Glenwood, IL). This reader operates in continuous-wave, cw, mode with a 1-s illumination read-period. In cw mode the read-light intensity is constant for the read period. The reader was operated in its "hardware test" modality, using the low-intensity LED-beam for preirradiation and postirradiation measurements. This allowed repeated readings of an OSLD with a signal decrease per reading of 0.05%.[19]

The Nanodots used in this work were used according to previously published protocols.[19,39] All Nanodots were preirradiated by 10 kGy, which linearized their response to dose. The detectors were used repeatedly and were optically reset after an exposure. After an irradiation, readings were not made for at least 8 min to allow the transient signal to decay away and were made within 1 h to avoid signal fading. Nanodots were read four times, and the average was reported as the reading. For a 100 cGy irradiation typical readings are as follows: 113290, 112428, 113240, 112451, average 112852 counts, standard deviation 477 counts, and coefficient of variation 0.42%. The dose was calculated as follows:

$$D = S \times (Ra - Rb) \quad (4)$$

where S is the dose sensitivity of the Nanodot, Rb is the reading immediately before the irradiation, and Ra is the reading after the irradiation. Rb must be established before each irradiation since it slowly increases[39] during storage in the dark. S is established by irradiating the Nanodot with a known dose, usually 20 cGy, and reading its response

$$S = (Ra20 - Rb)/20cGy$$

where Ra20 is the reading for a 20 cGy exposure delivered in the geometry shown in Fig. 1. Typical Ra20 readings are as follows: 37882, 37445, 37701, 37636, average 37666 counts, standard deviation 180 counts, and coefficient of variation 0.48%. After each exposure, each Nanodot is optically reset and a current S value is determined.

The second type of detector was a P-type semiconductor, designated as an SI4 (Standard Imaging, Madison, WI). These diodes[40] have less than 3.3% change in sensitivity for all incident angles and a water-equivalent buildup of 0.8 mm. All diode outputs were measured with a clinic built amplifier that integrated charge during radiation exposures or with a Max4000 electrometer (Standard Imaging, Madison, WI) operated in the zero-bias mode.

In the measurements carried out in this work the deviation from the dose-per-pulse value under reference conditions is at most −10.5% to +8.5%. The Nanodots have been shown[19] to have no change in sensitivity, within experimental error, for a 388-fold change in dose-per-pulse. The diodes[40] used in these measurements have a 1.6% change in sensitivity for a 260-fold change in dose-per-pulse. Under these conditions, dose-per-pulse corrections for either device will be less than 6×10^{-4} and are ignored.

Buildup caps for these detectors were fabricated out of M3 (Ref. 41) (Paraffin:magnesium-oxide:calcium-carbonate = 76.92 gm:22.4 gm:0.7 gm), a water-equivalent

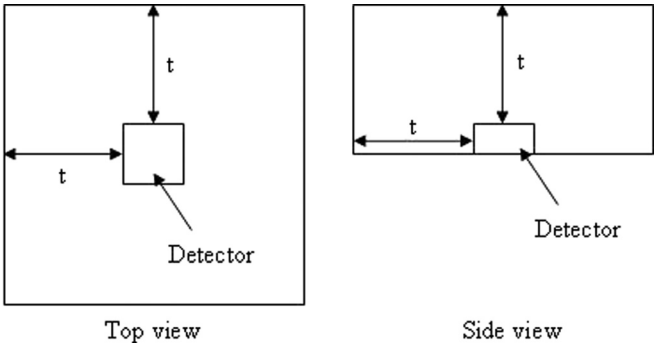

FIG. 2. A drawing of the geometry of the buildup caps that were fabricated in the clinic. The wall thickness, t, is dependent on wall material as shown in Table I. The detector slot is 10 mm × 10 mm × 2 mm for the Nanodots and 7 mm wide by 2 mm deep for the diode.

material, and sheet-metal stock of Al, Cu, and Pb. The caps were shaped as blocks as shown in Fig. 2 with wall thickness as shown in Table I. Commercially available hemispherical buildup caps, made of Plastic Water (CIRS, Inc., Norfolk, VA) and brass (Landauer, Inc., Glenwood, IL) were designed for use with Nanodots and were also used. Characteristics of these caps are shown in Table II. When in use, the detector is placed on the surface of the phantom with the buildup cap over it towards the source of radiation. This is the same phantom as shown in Fig. 1. Calibrations and measurements were done at different times.

Dose calculations for radiation delivery to a solid water slab (Standard Imaging, Madison, WI) were carried out with the XiO treatment planning system (CMS/Elekta, Stockholm). Calculations were made with heterogeneity corrections and the solid water had a mass density of 1.05 g/cm^3.

IV. RESULTS

Measurements of dose from a 6 MV beam with a Nanodot are shown in Fig. 3. In this graph and subsequent graphs in this paper, the data are shown as a ratio of Nanodot or diode response to the calculated dose that would be delivered to the depth of maximum dose if the detector was not present. The ratio of the detector response and calculated dose are normalized to 1 for a field size of 10 cm × 10 cm. This plotted ratio is the inverse of the C_{FS} defined in Eq. (3). Large dose ratios in these plots correlate with C_{FS} much less than unity being needed.

The data in Fig. 3 clearly show that with no buildup cap a change in dose ratio as large as 200% for a field-size change from 3 cm × 3 cm to 30 cm × 30 cm occurs. This corresponds to a C_{FS} as large as 1.33 to as small as 0.69. Figure 3 also shows that the change in dose ratio is reduced to about 4% when buildup caps with wall thickness equal to the depth of maximum dose is used. The brass hemisphere cap with a 4-mm wall thickness is about twice the thickness needed for dmax at 6 MV (see Table II). Nevertheless, this buildup cap results in the same magnitude of dose ratio as found with the other caps with dmax wall thickness. It can also be seen in Fig. 3 that the buildup cap fabrication material has little or no effect.

TABLE I. Characteristics of the materials used to fabricate buildup caps and the consequent wall thickness of these caps.

Material	Mass density (g/cm^3)	X-ray energy (MeV)	Wall thickness t (mm)
M3	1.05	6	15
M3	1.05	15	30
Al	2.69	6	5.5
Al	2.69	15	11.0
Cu	8.94	6	1.7
Cu	8.94	15	3.4
Pb	11.33	6	0.9
Pb	11.33	15	1.8

Measurements of dose from a 15 MV beam with a Nanodot are shown in Fig. 4. For the 15 MV beam with no buildup cap, the change in dose ratio is as large as 300% for a field-size change from 3 cm × 3 cm to 30 cm × 30 cm. Data are shown in Fig. 4 when a buildup cap made of plastic water, which has a 15 mm radius, is used for 15 MV measurements. This cap is not adequate to provide buildup for 15 MV x-rays and a change in dose ratio as large as 9% occurs. In this case the dose ratio has the opposite change with field size as seen for a buildup cap of adequate wall thickness. Figure 4 shows that the dose ratio becomes about 5% when buildup caps with wall thickness equal to dmax are used. Again, it is observed that the fabrication material of the buildup cap does not have a large effect on the dose ratio.

The reliability of Nanodot measurements is demonstrated by repeated measurements made with different detectors. These data are shown in Table III. Measurements with Nanodots that are individually calibrated and optically reset between each use have coefficients of variation of 0.6% or less. This level of precision can be achieved with 6 or 15 MV x-rays for full phantom geometry, as shown in Fig. 1, or with Nanodots placed at the phantom surface with appropriate buildup caps.

Measurements of dose from a 6 MV beam with a diode are shown in Fig. 5. The data in Fig. 5 clearly shows that

TABLE II. Characteristics of the commercially available hemispherical buildup caps and their wall thickness above the Nanodot.

Material	Mass density (g/cm^3)	X-ray energy (MV)	Required wall thickness for D_{dmax}, (mm)	Actual wall thickness above the Nanodot (mm)
Plastic water	1.03	6	15	14
Plastic water	1.03	15	29	14
Brass	8.5	6	1.8	4
Brass	8.5	15	3.5	4

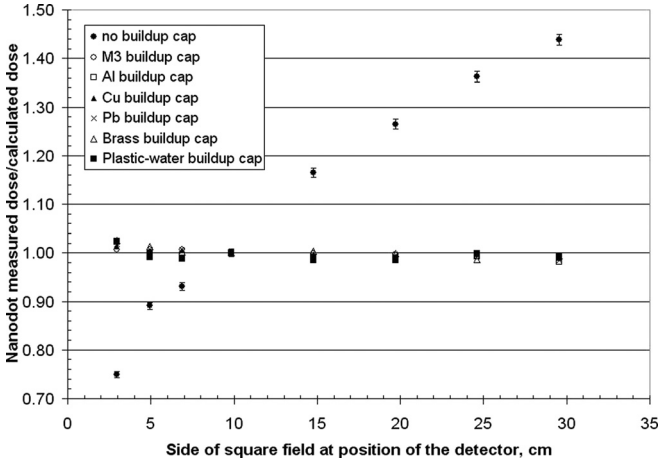

FIG. 3. The ratio of the Nanodot response to the calculated dose at the depth of maximum dose versus the field size at the position of the detector. The ratio of the detector response and calculated dose are normalized to 1 for a field size of 10 cm × 10 cm. For 6 MV x-rays, the depth of maximum dose is 1.5 cm, the detector is on the surface of a slab of solid water, the SSD is 98.5 cm, and the detector is covered with build up caps fabricated from the indicated materials. The calculated dose is determined with a treatment planning system. Typical error bars for one standard deviation are shown on the "no buildup cap data." These standard deviations are based on four repeats of the experiment.

with no buildup cap a change in dose ratio as large as 37% for a field-size change from 3 cm × 3 cm to 30 cm × 30 cm occurs. Figure 5 shows that the change in dose ratio becomes about 6% when a buildup cap is used that has a wall thickness equal to the depth of maximum dose. If a buildup cap that is designed for use with 15 MV x-ray is used, which has walls that are twice as thick as necessary (see Table I), then it results in the same magnitude of dose ratio. As already observed for Nanodots, Fig. 5 shows that the buildup cap fabrication material is not of major importance.

Measurements of dose from a 15 MV beam with a diode are shown in Fig. 6. For the 15 MV beam the change in dose

TABLE III. Repeated measurements with Nanodots. Six different detectors were used and each was calibrated and optically reset as described in Sec. III. The measurements were made for 100 MU delivered with the Nanodot under a buildup cap and a source to detector distance of 100 cm.

Nanodot	Dose measured with full phantom (cGy)	Dose measured with plastic-water buildup cap described in Table II (cGy)
6 MV x-rays		
1	100.4	96.5
2	99.4	96.6
3	99.6	96.2
4	99.4	97.3
5	100.2	96.5
6	100.1	95.4
Average (cGy)	99.8	96.4
Standard deviation (cGy)	0.4	0.6
Coefficient of variation (%)	0.4	0.6
15 MV x-rays		
1	100.4	104.2
2	100.2	105.3
3	101.1	105.4
4	100.9	105.4
5	100.7	106.0
6	101.5	104.9
Average (cGy)	100.8	105.2
Standard deviation (cGy)	0.5	0.6
Coefficient of variation (%)	0.5	0.6

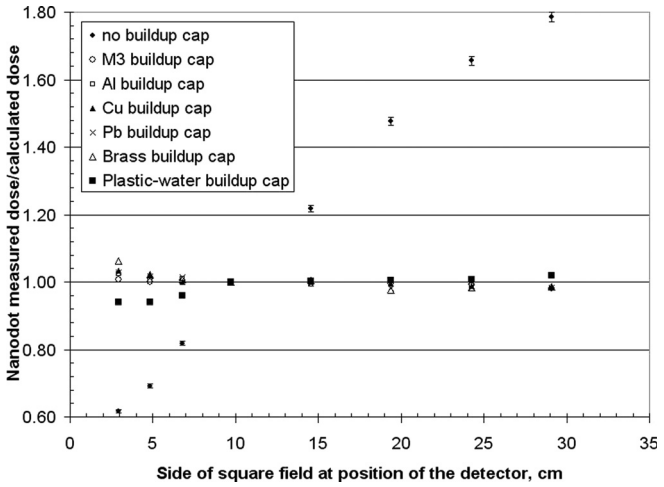

FIG. 4. The ratio of the Nanodot response to the dose at the depth of maximum dose versus the field size at the position of the detector. The ratio of the detector response and calculated dose are normalized to 1 for a field size of 10 cm × 10 cm. These data are for a 15 MV x-ray beam, which has a depth of maximum dose is 3.0 cm, the detector is on the surface of a slab of solid water, SSD to the surface of the solid water is 97.0 cm, and the detector is covered with build up caps fabricated from the indicated materials. The calculated dose is determined with a treatment planning system. Typical error bars for one standard deviation are shown on the "no buildup cap data." These standard deviations are based on four repeats of the experiment.

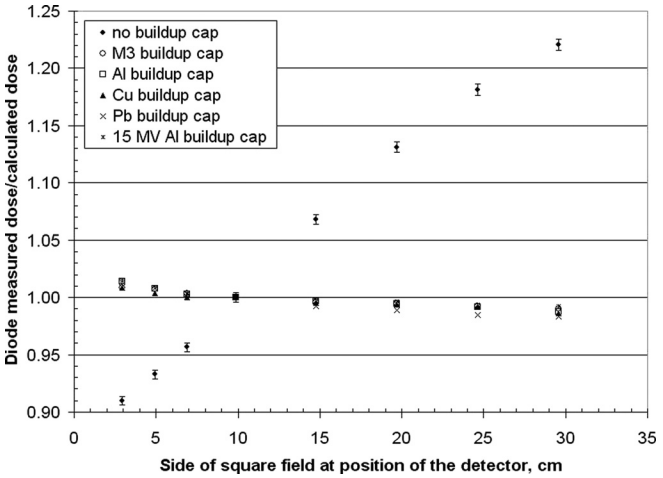

FIG. 5. The ratio of the diode response to the dose at the depth of maximum dose versus the field size at the position of the detector. The ratio of the detector response and calculated dose are normalized to 1 for a field size of 10 cm × 10 cm. X-rays of 6 MV are used, the depth of maximum dose is 1.5 cm, the detector is on the surface of a slab of solid water, SSD to the surface of the solid water is 98.5 cm, and the detector is covered with build up caps fabricated from the indicated materials. The calculated dose is determined with a treatment planning system. Typical error bars for one standard deviation are shown on the "no buildup cap data." These standard deviations are based on four repeats of the experiment.

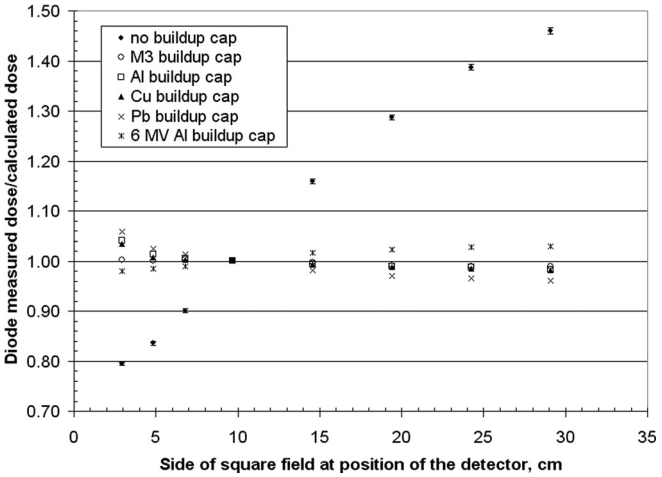

FIG. 6. The ratio of the diode response to the dose at the depth of maximum dose versus the field size at the position of the detector. The ratio of the detector response and calculated dose are normalized to 1 for a field size of 10 cm × 10 cm. These data are for a beam of 15 MV x-ray, which has a depth of maximum dose is 3.0 cm, the detector is on the surface of a slab of solid water, SSD to the surface of the solid water is 97.0 cm, and the detector is covered with build up caps fabricated from the indicated materials. The calculated dose is determined with a treatment planning system. Typical error bars for one standard deviation are shown on the "no buildup cap data." These standard deviations are based on four repeats of the experiment.

ratio with no buildup cap is as large as 80% for a field-size change from 3 cm × 3 cm to 30 cm × 30 cm. Data are shown in Fig. 6; when a buildup cap made of aluminum, which has a 15-mm wall thickness, a 6 MV buildup cap is used for 15 MV measurements. This cap is not adequate to provide buildup for 15 MV x-rays, and the change in dose ratio as large as 5% occurs. In this case the dose ratio has the opposite change with field size as seen for a buildup cap of adequate wall thickness. Figure 6 also shows that the change in dose ratio becomes about 5% when a buildup cap with wall thickness equal to the depth of maximum dose is used. It is also shown in Fig. 6, when a cap made of M3 is used, that the dose ratio remains near unity for field sizes below 10 cm × 10 cm. Again, it is observed that except for M3 the fabrication material of the buildup cap does not have a large effect on the dose ratio.

TABLE IV. The decrease in dose caused by an OSLD or a diode with or without its buildup cap. The dose was measured with a diode positioned at the depth of 1.5 cm for 6 MV and 3 cm for 15 MV x-rays, on the central axis of a 10 cm × 10 cm beam, with a source-to-detector distance of 100 cm.

Buildup cap material	6 MV x-rays (%)	15 MV x-rays (%)
OSLD only, no cap	0.3	0.2
OSLD, Al	4.6	5.8
OSLD, Cu	3.8	5.9
OSLD, Pb	4.6	6.2
OSLD, plastic-water cap	4.6	3.4
OSLD, brass cap	20.5	16.9
Diode only, no cap	1.4	0.7
Diode, Al	6.4	7.5
Diode, Cu	5.4	7.0
Diode, Pb	5.9	6.8

Placing a detector on the surface of a patient will perturb the dose delivered by attenuation and scatter of the beam. The magnitude of this effect was tested by measuring dose on the central axis of the beam at the depth of maximum dose with and without a detector and buildup cap in place. These results are shown in Table IV. For the detectors with no buildup caps, the diode is seen to have a larger attenuation than a Nanodot. This is expected since the intrinsic buildup of the diode[12] is larger than that of a Nanodot.[19] With buildup caps in place, the attenuation of dose remains at about 4%–7.5% except the brass hemispherical cap, which showed an attenuation of 20.5% for 6 MV x-rays. The high attenuation of the brass cap is expected since, as shown in Table II, its wall thickness is greater than dmax.

Tables V and VI show a comparison between calculated dose and dose measured with a Nanodot and a diode for 6 and 15 MV x-rays. The detectors with the appropriate buildup cap were positioned on the surface of a slab of solid water. The position of the solid water, its SSD, and the field size were

TABLE V. A comparison between the dose at 1.5 cm depth measured with a detector on the surface and the dose calculated with the treatment planning system. The x-ray beam used was 6 MV and a dose of 50 cGy was delivered to the depth of maximum dose at SSD of 98.5 cm with a 10 cm × 10 cm field. The detector was covered with an aluminum buildup cap. The C_{FS} values were obtained from the data in Figs. 3–6. The measured dose was corrected according to Eq. (1). The percent difference is calculated as follows: %Diff = 100 × (measured − calculated)/calculated. The indicated errors are standard deviations based on four repeats of the experiment.

Detector	SSD (cm)	Side length of a square field at the detector (cm)	C_{FS}	Calculated dose (cGy)	Measured dose (cGy)	%Diff.
Nanodot	88.5	4.4	0.985 ± 0.008	58.5	58.7 ± 0.6	0.25
Nanodot	98.5	4.9	0.988 ± 0.008	47.5	47.0 ± 0.5	−1.05
Nanodot	108.5	5.4	0.990 ± 0.008	39.3	39.2 ± 0.5	−0.38
Nanodot	88.5	26.6	1.010 ± 0.008	66.6	66.3 ± 0.6	−0.52
Nanodot	98.5	29.6	1.013 ± 0.008	54.0	54.5 ± 0.5	0.88
Nanodot	108.5	32.6	1.015 ± 0.008	44.7	45.0 ± 0.5	0.72
Diode	88.5	4.4	0.993 ± 0.008	58.5	58.1 ± 0.4	−0.72
Diode	98.5	4.9	0.992 ± 0.008	47.5	47.0 ± 0.3	−1.16
Diode	108.5	5.4	0.994 ± 0.008	39.3	38.8 ± 0.3	−1.28
Diode	88.5	26.6	1.011 ± 0.008	66.6	66.6 ± 0.4	0.04
Diode	98.5	29.6	1.013 ± 0.008	54.0	54.0 ± 0.4	0.00
Diode	108.5	32.6	1.015 ± 0.008	44.7	44.6 ± 0.3	−0.16

TABLE VI. A comparison between the dose at 3.0 cm depth measured with a detector on the surface and the dose calculated with the treatment planning system. The x-ray beam used was 15 MV. All other details are the same as in legend for Table V.

Detector	SSD (cm)	Side length of a square field at isocenter (cm)	C_{FS}	Calculated dose (cGy)	Measured dose (cGy)	%Diff.
Nanodot	87.0	4.4	0.993 ± 0.008	58.5	58.9 ± 0.6	0.68
Nanodot	97.0	4.9	0.995 ± 0.008	47.5	47.6 ± 0.5	0.14
Nanodot	107.0	5.4	0.997 ± 0.008	39.4	39.6 ± 0.5	0.5
Nanodot	87.0	26.1	1.015 ± 0.008	66.3	66.3 ± 0.6	0.05
Nanodot	97.0	29.1	1.020 ± 0.008	53.8	54.3 ± 0.5	0.96
Nanodot	107.0	32.1	1.024 ± 0.008	44.4	44.6 ± 0.4	0.35
Diode	87.0	4.4	0.980 ± 0.004	58.5	58.5 ± 0.4	−0.06
Diode	97.0	4.9	0.987 ± 0.004	47.5	47.7 ± 0.3	0.34
Diode	107.0	5.4	0.990 ± 0.004	39.4	39.5 ± 0.3	0.29
Diode	87.0	26.1	1.011 ± 0.004	66.3	65.8 ± 0.4	−0.80
Diode	97.0	29.1	1.013 ± 0.004	53.8	54.5 ± 0.4	1.30
Diode	107.0	32.1	1.015 ± 0.004	44.4	44.0 ± 0.3	−0.92

changed within common ranges used in clinical work. The differences between measured and calculated doses to depth dmax were found to be in a range of ±1.3% for 100 cGy. For the geometry in these measurements, the values for CF_{FS} were between 0.980 and 1.024.

V. DISCUSSION

In order to measure a dose in the patient, generally at a depth of maximum dose, by placing a detector on the surface of the patient, one is faced with a lack of buildup and scatter at the surface position compared to point inside the patient. A buildup cap, as the name implies, provides dose buildup and a partial amount of the scatter that occurs at depth dmax inside the patient. The C_{FS} corrects for the difference in scatter at the detector position versus the reference position. The data in Figs. 3–6 show how C_{FS} changes with field size at the position of the detector for different types of build up caps. For the Nanodot and diode detectors used in this work the results are qualitatively identical.

There has been only one report of OSLD use with buildup caps.[25] In this work it was shown that a 2-mm-thick, stainless-steel, cap could be used to measure dose at dmax depth for Co-60 and 6 MV x-rays. No analysis of different types of caps or effects of field size was made in this report.

Earlier work with diodes has been reported for a variety of buildup caps and is summarized in Table VII. The results reported here are in good agreement with these earlier reports. When the buildup cap is thick enough for a measured energy the $C_{FS}(30\times30)/C_{FS}(5\times5)$ is greater than unity by 3%–5%. When the buildup cap is too thin for a measured energy the $C_{FS}(30\times30)/C_{FS}(5\times5)$ is greater than unity by 10%–20%.

The use of a detector with no buildup cap is the correct way to measure dose on the surface of the patient but it is an unsuitable way to measure dose at other depths in the patient. The data in Figs. 3–6 show that no buildup cap or an inadequate buildup cap will result in field-size correction factors that are large in magnitude and rapidly changing with field size. Use of such large, highly variable, correction factors will result in poor accuracy in the measured dose. It is also of interest that for no or inadequate buildup caps the ratio increases with field size. This is because without adequate buildup the detector is exposed to contamination electrons, which become more prominent with increased field size and beam energy.[31,32,42–45]

The data in Figs. 3 and 5 show that a buildup cap with wall thickness greater then dmax thickness for a particular energy beam results in a C_{FS} that is the same as found with a dmax thick buildup cap. The use of such a cap, with wall

TABLE VII. A summary of a sample of published data on C_{FS} using a variety of diodes and radiation beams.

$C_{FS}(30\times30)/C_{FS}(5\times5)$	Radiation beam	Buildup cap	Reference
0.995	6 MV x-rays	0.75-mm steel and 4-mm polyvinylchloride	1
1.00–0.982	4 and 8 MV x-rays	2.2-mm stainless steel and 2.8-mm epoxy	49
1.158	25 MV x-rays	20-mm water-equivalent	35
0.995–1.001	8 MV x-rays	2.2-mm stainless steel and 2.8-mm epoxy	14
1.020	18 MV x-rays	2-mm stainless steel and copper	28
1.072	18 MV x-rays	1-mm tantalum	29
0.984	18 MV x-rays	0.5-mm polyacetal and 1.6-mm tungsten and 2.4-mm epoxy	29
1.036	6 MV x-rays	1.6-mm brass	50
1.022	6 MV x-rays	2.2-mm brass	50
0.987	8 MV x-rays	2.2-mm stainless steel and 2.8-mm epoxy	30
1.028	18 MV x-rays	2.2-mm stainless steel and 2.8-mm epoxy	30

thickness that is greater than needed, is discouraged since it will result in unnecessary beam attenuation during the measurement.

It is interesting for buildup caps constructed with adequate wall thickness that the C_{FS} is found to be independent on the atomic number on the fabrication material (Figs. 3–6). In earlier work[31] it was shown that the measurement of collimator scatter with a columnar-miniphantom is dependent on the atomic number of the fabrication material of the miniphantom. The explanation was that the attenuation and scatter in the miniphantom, which has a long cylindrical geometry, were large in magnitude and had dependence on the atomic number of the fabrication material. The buildup caps used here do not have the long, narrow geometry of a miniphantom, and the results presented here indicate a minimal effect of the atomic number of the material used to fabricate the buildup caps. Only a small effect is expected as the dominant photon–electron interaction at 6 and 15 MV is the Compton effect, which depends upon the electron density (ρ).[46]

The use of a low-density material such as M3 certainly works to give a buildup cap with reasonable C_{FS} values (Figs. 3–6). However, the resulting buildup cap has the inconvenience of quite large dimensions, as shown in Table I. One of the consequences of this is seen in Figs. 4 and 6. The C_{FS} does not decrease for fields with side length less than 10 cm. This occurs because for 15 MV beams, the M3 buildup cap is over 6 cm in width and the perimeters of the smaller fields are completely inside the buildup cap. In other words, the buildup cap is so large that it acts as a slab phantom that provides complete scatter for the small fields.

When placing a detector with its buildup cap on the surface of a patient two perturbation of patient dose occur.[47] The surface dose will increase since the detector and its cap will act as buildup material. For dose at greater depth, the detector and its cap will attenuate dose. The extent of perturbation of patient dose by a detector with a buildup cap has been reported to be from 1% to 8% (Refs. 12, 14, and 28) and up to 13% (Ref. 48) for diodes with cylindrical buildup caps made of tungsten. In this work, the extent of perturbation by a Nanodot and a diode with and without their buildup caps was measured and is shown in Table IV. There is about 20% more attenuation by diodes with buildup caps than Nanodots with buildup caps. From the results in Table IV, one must conclude that daily use of a detector with its buildup cap is ill advised. However, a single use at the beginning of a course of treatment or of a field cone-down is a procedure that would cause minimal perturbation of delivered dose.

When correction factors are carefully determined and applied to measurements made on the surface, then very good measures of the dose at depth dmax can be made. This is shown in Tables V and VI for 6 and 15 MV x-rays delivered over the typical range of clinical field sizes and SSDs. Clearly, the small differences that were observed between measured and calculated dose were acceptable for clinical work and could only be accomplished if the CF_{FS} values were applied to the detector measurements.

VI. CONCLUSIONS

OSLDs and diodes with appropriate buildup caps can be used to measure dose on the surface of a patient and predict the delivered dose to depth dmax in a range of ±1.3% for 100 cGy. The buildup cap: can be fabricated from any material examined in this work, is best with wall thickness dmax, and causes a perturbation to the delivered dose of 4%–7% when the wall thickness is dmax. OSLDs and diodes with buildup caps can both give accurate measurements of delivered dose.

[a]Electronic mail: pjursinic@wmcc.org

[1]G. Leunens, J. Van Dam, A. Dutreix, and E. Van Der Shueren, "Quality assurance in radiotherapy by in vivo dosimetry. 1. Entrance dose measurements, a reliable procedure," Radiother. Oncol. **17**, 141–151 (1990).
[2]G. Leunens, J. Verstraete, A. Dutreix, and E. van der Schueren, "Assessment of dose inhomogeneity at target level by in vivo dosimetry: Can the recommended 5% accuracy in the dose delivered to the target volume be fulfilled in daily practice?" Radiother. Oncol. **25**, 242–250 (1992).
[3]J. H. Lanson, M. Essers, G. J. Meijer, A. W. H. Minken, G. J. Uiterwaal, and B. J. Mijnheer, "In vivo dosimetry during conformal radiotherapy: Requirements for and findings of a routine procedure," Radiother. Oncol. **52**, 51–59 (1999).
[4]M. Essers and B. J. Mijnheer, "In vivo dosimetry during external photon beamradiotherapy," Int. J. Radiat. Oncol. Biol. Phys. **43**, 245–249 (1999).
[5]P. A. Jursinic, "Implementation of an in vivo diode dosimetry program and changes in diode characteristics over a four-year clinical history," Med. Phys. **28**, 1718–1726 (2001).
[6]G. J. Kutcher, L. Coia, M. Gillin, W. F. Hanson, S. Leibel, R. J. Morton, J. R. Palta, J. A. Purdy, L. E. Reinstein, G. K. Svensson, M. Weller, and L. Wingfield, "Comprehensive QA for radiation oncology: Report of AAPM Radiation Therapy Committee Task Group 40," Med. Phys. **21**, 581–618 (1994).
[7]F. H. Attix, "Integrating dosimeters," *Introduction to Radiological Physics and Radiation Dosimetry* (John Wiley & Sons, New York, 1986), Chap. 14, pp. 395–437.
[8]J. Van Dam and G. Marinello, *ESTRO Booklet on Physics for Clinical Radiotherapy No. 1* (Garant, Leuven-Apeldoorn, 1994).
[9]E. Yorke, R. Alecu, L. Ding, R. Boissoneault, D. Fontenla, A. Kalend, D. Kaurin, M. E. Masterson-McGary, G. Marinello, T. Matzen, A. Saini, J. Shi, W. Simon, T. C. Zhu, X. R. Zhu, G. Rikner, and G. Nilsson, "Diode in vivo dosimetry for patients receiving external beam radiation therapy," Report of Task Group 62 of the Radiation Therapy Committee (Medical Physics Publishing, Madison, WI, 2005).
[10]S. Tavernier, A. Gektin, B. Grinyov, and W.W. Moses, *Radiation Detectors for Medical Applications* (Springer, Dordecht, 2005).
[11]M. Soubra, J. Cygler, and G. Mackay, "Evaluation of a dual bias dual metal–oxide–silicon semiconductor field effect transistor detector as radiation detector," Med. Phys. **21**, 567–572 (1994).
[12]G. Rikner and E. Grusell, "Effect of radiation damage on p-type silicon detectors," Phys. Med. Biol. **28**, 1261–1267 (1983).
[13]G. Rikner and E. Grusell, "Patient dose measurements in photon fields by means of silicon semiconductor detectors," Med. Phys. **14**, 870–873 (1987).
[14]T. Loncol, J. L. Greffe, S. Vynckier, and V. Scalliet, "Entrance and exit dose measurements with semiconductors and thermoluminescent dosemeters: A comparison of methods and in vivo results," Radiother. Oncol. **41**, 179–187 (1996).
[15]M. S. Akselrod, V. S. Kortov, D. J. Kravetsky, and V. I. Gotlib, "High sensitivity thermoluminescent anion-defective α-Al_2O_3:C crystal detectors," Radiat. Prot. Dosim. **32**, 15–20 (1990).
[16]M. S. Akselrod, V. S. Kortov, and E. A. Goreleva, "Preparation and properties of α-Al_2O_3:C," Radiat. Prot. Dosim. **47**, 159–164 (1993).
[17]A. J. J. Bos, "High sensitivity thermoluminescence dosimetry," Nucl. Instrum. Methods Phys. Res. B **184**, 3–28 (2001).
[18]L. Bøtter-Jensen, N. Agersnap-Larsen, B. G. Markey, and S. W. S. McKeever, "Al_2O_3:C as a sensitive OSL dosimeter for rapid assessment of environmental photon dose rate," Radiat. Meas. **27**, 295–298 (1997).

[19]P. Jursinic, "Characterization of optically stimulated luminescent dosimeters, OSLDs, for clinical dosimetric measurements," Med. Phys. **34**, 4594–4604 (2007).
[20]S. D. Miller and M. K. Murphy, "Technical performance of the Luxel α-Al_2O_3:C optically stimulated luminescence dosimeter element at radiation oncology and nuclear accident dose levels," Radiat. Prot. Dosim. **123**, 435–442 (2007).
[21]V. Schembri and B. J. M. Heijmen, "Optically stimulated luminescence (OSL) of carbon-doped aluminum oxide (Al_2O_3:C) for film dosimetry radiotherapy," Med. Phys. **34**, 2113–2118 (2007).
[22]E. G. Yukihara and S. W. S. McKeever, "Optically stimulated luminescence (OSL) dosimetry in medicine," Phys. Med. Biol. **53**, R351–R379 (2008).
[23]E. G. Yukihara, G. Mardirossian, M. Mirzasadeghi, S. Guduru, and S. Ahmad, "Evaluation of Al2O3:C optically stimulated luminescence (OSL) dosimeters for passive dosimetry of high-energy photon and electron beams in radiotherapy," Med. Phys. **35**, 260–269 (2008).
[24]C. S. Reft, "The energy dependence and dose response of a commercial optically stimulated luminescent detector for kilovoltage photon, megavoltage photon, and electron, proton, and carbon beams," Med. Phys. **36**, 1690–1699 (2009).
[25]A. Viamonte, L. A. R. da Rosa, L. A. Buckley, A. Cherpak, and J. E. Cygler, "Radiotherapy dosimetry using a commercial OSL system," Med. Phys. **35**, 1261–1266 (2008).
[26]J. E. Cygler and E. G. Yukihara, "Optically stimulated luminescence (OSL) dosimetry in radiotherapy," in *AAPM 2009 Summer School, Clinical Dosimetry Measurements in Radiotherapy*, edited by D. W. O. Rogers and J. Cygler (Medical Physics Publishing, Madison, WI, 2009).
[27]G. Marinello, *Handbook of Radiotherapy Physics*, edited by P. Mayles, J. C. Rosenwald, and A. Nahum (CRC, Boca Raton/Taylor and Francis, New York, 2007), pp. 303–320.
[28]D. Georg, B. De Ost, M. T. Hoornaert, P. Pilette, J. Van Dam, M. Van Dycke, and D. Huyskens, "Build-up modification of commercial diodes for entrance dose measurements in 'higher energy' photon beams," Radiother. Oncol. **51**, 249–256 (1999).
[29]N. Jornet, M. Ribas, and T. Eudaldo, "Calibration of semiconductor detectors for dose assessment in total body irradiation." Radiother. Oncol. **38**, 247–251 (1996).
[30]G. T. Meijer, A. W. H. Minken, K. M. van Ingen, B. Smulders, H. Uiterwaal, and B. J. Mijnheer, "Accurate in vivo dosimetry of a randomized trial of prostate cancer irradiation," Int. J. Rad. Oncol. Biol. Phys. **49**, 1409–1418 (2001).
[31]P.A. Jursinic, "Measurement of head scatter factors of linear accelerators with columnar miniphantoms," Med. Phys. **33**, 1720–1728 (2006).
[32]J. J. M. van Gasteren, S. Heukelom, H. J. van Kleffens, R. van der Laarse, J. L. M. Venselaar, and C. F. Westermann, "The determination of phantom and collimator scatter components of the output of megavoltage photon beams: Measurements of the collimator scatter part with a beam-coxial narrow cylindrical phantom," Radiother. Oncol. **20**, 250–257 (1991).
[33]M. Essers, J. H. Lanson, and B. J. Mijnheer, "In vivo dosimetry during conformal therapy of prostatic cancer," Radiother. Oncol. **29**, 271–279 (1993).
[34]M. Essers, R. Keus, J. H. Lanson, and B. J. Mijnheer, "Dosimetric control of conformal treatment of parotid gland tumors," Radiother. Oncol. **32**, 154–162 (1994).
[35]D. P. Fontenla, R. Yaparpalvi, C. S. Chui, and E. Briot, "The use of diode dosimeters in quality improvement of patient care in radiation therapy," Med. Dosim. **4**, 235–241 (1996).
[36]P. R. Almond, P. J. Biggs, B. M. Coursey, W. F. Hanson, M. S. Huq, R. Nath, and D. W. O. Rogers, "AAPM's TG-51 protocol for clinical reference dosimetry of high-energy photon and electron beams," Med. Phys. **26**, 1847–1870 (1999).
[37]L. Bøtter-Jensen, S. W. S. McKeever, and A. G. Wintle, *Optically Stimulated Luminescence Dosimetry* (Elsevier, The Netherlands, 2003).
[38]E. G. Yukihara and S. W. S. McKeever, *Optically Stimulated Luminescence: Fundamentals and Applications* (John Wiley & Sons, West Sussex, UK, 2011).
[39]P. Jursinic, "Changes in optically stimulated luminescent dosimeter (OSLD) dosimetric characteristics with accumulated dose," Med. Phys. **37**, 132–140 (2010).
[40]P. Jursinic, "Angular dependence of dose sensitivity of surface diodes," Med. Phys. **36**, 2165–2171 (2009).
[41]D. R. White, "Tissue substitutes in experimental radiation physics," Med. Phys. **5**, 467–479 (1978).
[42]T. N. Padikal and J. A. Deye, "Electron contamination of a high-energy x-ray beam," Phys. Med. Biol. **23**, 1086–1092 (1978).
[43]B. R. Thomadsen, S. Kubsad, B. R. Paliwal, S. Shahabi, and T. R. Mackie, "On the cause of the variation in tissue-maximum ration values with source-to-detector distance," Med. Phys. **20**, 723–727 (1993).
[44]P. A. Jursinic and B. R. Thomadsen, "Measurements of head-scatter factors with cylindrical build-up caps and columnar miniphantoms," Med. Phys. **26**, 512–517 (1999).
[45]P. A. Jursinic and T. R. Mackie, "Characteristics of secondary electrons produced by 6, 10 and 24 MV x-ray beams," Phys. Med. Biol. **41**, 1499–1509 (1996).
[46]F. H. Attix, "Gamma and x-ray interactions in matter," *Introduction to Radiological Physics and Radiation dosimetry* (John Wiley and Sons, New York, 1986), Chap. 7, pp. 124–159.
[47]B. Nilsson, B. I. Ruden, and B. Sorcini, "Characteristics of silicon diodes as patient dosimeters in external radiation therapy," Radiother. Oncol. **11**, 279–288 (1988).
[48]R. Alecu, J. J. Feldmeier, and M. Alecu, "Dose perturbations due to *in vivo* dosimetry with diodes," Radiother. Oncol. **42**, 289–291 (1997).
[49]S. Heukelom, J. H. Lanson, and B. J. Mijnheer, "Comparison of entrance and exit dose measurements using ionization chambers and silicon diodes," Phys. Med. Biol. **36**, 47–59 (1991).
[50]X. R. Zhu, "Entrance dose measurements for in-vivo diode dosimetry: Comparison of correction factors for two types of commercial silicon diode detectors," J. Appl. Clin. Med. Phys. **1**, 100–107 (2000).